

# Appendix C

## Supplemental: The Kinetics of Toehold-Mediated Four-way Branch Migration<sup>0</sup>

### C.1 Experimental Details

Sequences for experiments discussed in the main text can be found in Table C.1. Colors correspond to the domains found in Figure 5.1. At least three traces for each toehold combination were analyzed (Figures C.1, C.2, C.3, C.4, C.5, C.6, C.7). Each toehold combination was investigated with at least two different concentration sets. The solid lines show fluorescence data, dotted lines show simulated fits for  $k_1$  or  $k_2$ , and the gray dotted line shows the average fit simulation at each concentration (fitting method is explained below). Concentrations investigated can be found in Tables C.4 and C.3.

---

<sup>0</sup>This work was coauthored by Nadine Dabby, Ho-Lin Chen, Joseph Schaeffer, & Erik Winfree\* and is currently in submission [Dabby et al., 2013] with the following contributions: all experiments were performed by N. D.; trajectory simulations were performed by J.S.; analysis was performed by N. D., H-L.C., J.S with supervision by E.W. Experimental design and manuscript was done with input from all authors.

Table C.1: Experiment sequences

reporter1-m16	\5IAbRQ\ -ACCGCACGTCCACGGTGTCGC-ACCCACTCCTTCTCAA
reporter1-m6	\5IAbRQ\ -ACCGCACGTCCACGGTGTCGC-ACCCAC
reporter2	GCTAAC-GCGACACCGTGGACGTGCGGT-\3Rox\
complex-m16	TTGAGAAGGAGTGGGT-GCGACACCGTGGACGTGCGGT
complex-m6	GTGGGT-GCGACACCGTGGACGTGCGGT
complex-m4	GGGT-GCGACACCGTGGACGTGCGGT
complex-m2	GT-GCGACACCGTGGACGTGCGGT
complex-m0	GCGACACCGTGGACGTGCGGT
complex-n6	ACCGCACGTCCACGGTGTCGC-GTTAGC
complex-n4	ACCGCACGTCCACGGTGTCGC-GTTA
complex-n2	ACCGCACGTCCACGGTGTCGC-GT
complex-n0	ACCGCACGTCCACGGTGTCGC
m-displace	GTGGGT-GCGACACCGTGGACGTGCGGT
n-displace	ACCGCACGTCCACGGTGTCGC-GTTAGC

Fitted Four-way Unimolecular Rates		
toehold length	average (sec <sup>-1</sup> )	standard deviation
$m = 16, n = 0$	$4.4 \times 10^{-4}$	$4.5 \times 10^{-5}$
$m = 16, n = 2$	$1.4 \times 10^{-3}$	$2.2 \times 10^{-4}$
$m = 16, n = 4$	$1.9 \times 10^{-3}$	$4.5 \times 10^{-4}$
$m = 16, n = 6$	$1.2 \times 10^{-3}$	$4.9 \times 10^{-4}$

Table C.2: Unimolecular rates ( $k_2$ ) determined by mean squared error fitting to experimental traces. We assume that the bimolecular rate is  $3 \times 10^6 \text{ mol}^{-1} \text{ sec}^{-1}$ .

Table C.3: Four-way Branch Migration Long-Toehold Experimental Concentrations

toehold length	Reporter concentration	Complex concentration
m = 16, n = 0	0.1 nM	0.5 nM
	0.25 nM	1 nM
	1 nM	5 nM
	20 nM	100 nM
m = 16, n = 2	0.1 nM	0.5 nM
	0.25 nM	1 nM
	1 nM	5 nM
	20 nM	100 nM
m = 16, n = 4	0.1 nM	0.5 nM
	0.25 nM	1 nM
	1 nM	5 nM
	20 nM	100 nM
m = 16, n = 6	0.1 nM	0.5 nM
	0.25 nM	1 nM
	1 nM	5 nM
	20 nM	100 nM

Table C.4: Four-way Branch Migration Experimental Concentrations

toehold length	Reporter concentration	Complex concentration
m = 0, n = 0	120 nM	3 $\mu$ M
	250 nM	3 $\mu$ M
m = 0, n = 2	120 nM	3 $\mu$ M
	250 nM	3 $\mu$ M
m = 0, n = 4	120 nM	3 $\mu$ M
	250 nM	3 $\mu$ M
m = 0, n = 6	120 nM	1 $\mu$ M
	250 nM	1 $\mu$ M
m = 2, n = 0	120 nM	3 $\mu$ M
	250 nM	3 $\mu$ M
m = 2, n = 2	120 nM	3 $\mu$ M
	250 nM	3 $\mu$ M
m = 2, n = 4	120 nM	2 $\mu$ M
	250 nM	2 $\mu$ M
m = 2, n = 6	25 nM	200 nM
	50 nM	200 nM
m = 4, n = 0	120 nM	2 $\mu$ M
	250 nM	2 $\mu$ M
m = 4, n = 2	120 nM	1 $\mu$ M
	250 nM	1 $\mu$ M
m = 4, n = 4	25 nM	200 nM
	50 nM	200 nM
m = 4, n = 6	0.5 nM	1 nM
	0.5 nM	2.5 nM
	2.5 nM	2.5 nM
m = 6, n = 0	50 nM	1.5 $\mu$ M
	100 nM	1.5 $\mu$ M
m = 6, n = 2	0.5 nM	5 nM
	2.5 nM	5 nM
m = 6, n = 4	0.5 nM	1 nM
	0.5 nM	2 nM
	0.5 nM	2.5 nM
	0.5 nM	5 nM
	0.5 nM	10 nM
	2.5 nM	2.5 nM
m = 6, n = 6	0.5 nM	1 nM
	0.5 nM	2.5 nM
	2.5 nM	2.5 nM

## C.2 Modeling and Sample Code

In order to determine  $k_2$  we designed reaction complexes with a 16-basepair toehold. We assumed  $k_1 = k_f = 3 \times 10^6$ , a value taken from [Zhang and Winfree, 2009], due to the length of the toeholds. We then fit a  $k_2$  value to each trace in MATLAB by minimizing the mean squared error of our fit function to the data. Sample code of the main function call for trace one of the  $m=16$ ,  $n=2$  data set follows:

```
% k0 is an initial estimate of k1;
k0 = log(0.0004);
[estimated_k] = fminunc(@err_func_m16n2v1, k0);
```

The error function *err\_func\_m16n2v1* follows:

```
function err_func = err_func_m16n2v1(input)

% x-axis = over-all time
% m_n = spectrofluorimeter read-out
% start_conc = limited reactant concentration
% offset = start time
% index_offset = index into offset time in the x-axis matrix
% baseline = low fluorescence level
% max = high fluorescence level
% end_index = end of the fit region

index_offset1 = 7;
offset1 = 300;
m_n1 = cleanm16n0246v1(:,3);
xaxis1 = cleanm16n0246v1(:,1);
baseline1 = min(m_n1);
max1 = max(m_n1);
max1b = max1;
start_conc1 = 20 * 10^(-9);
data = [xaxis1, m_n1];
end_index = size(data, 1);
k = exp(input(1));
```

```

err_func = 0;
options = odeset('MaxStep',100,'refine',1e-10,'InitialStep',100,'RelTol',1e-10,'AbsTol',1e-10);
datasize = size(data, 1);
t = data(index_offset1:datasize,1)-offset1;
y0 = [start_conc1*(max1b-baseline1)/(max1-baseline1), 0, 0, k];
[t, y2] = ode45(@fmin_toehold_norm_1, t, y0, options);
ye = y2(:,3);

for i = index_offset1:(end_index - index_offset1) //cutting off the displace
    strand reaction at the end
    err_func = err_func + ((ye(i-(index_offset1 -1)) - (data(i, 2) - baseline1)
        /(max1-baseline1)*start_conc1)^2)*1e17; %min square difference of sim -
        data
end

```

After finding the mean  $k_2$  values for all long-toehold experiments (Figure C.1), we found a disparity between the open (one toehold connecting the complexes) and closed (both toeholds connecting the complexes) cases of toehold-mediated four-way branch migration. All other traces were fit exactly as above, except that we assumed the  $k_2^{open}$  and  $k_2^{closed}$  values to be those calculated above, and we instead fit  $k_1$ .

All traces that did not reach a completion level of 20% within 24 hours were fit linearly using the polyfit function in Matlab. Sample code from one of the ( $m = 0, n = 2$ ) data set follows:

```

function [slope] = polyfit_m0n2v1()

% x-axis = over-all time
% m_n = spectrofluorimeter read-out
% start_conc = limited reactant concentration
% offset = start time
% index_offset = index into offset time in the x-axis matrix
% baseline = low fluorescence level
% max = high fluorescence level

```

```

% end_index = end of the fit region

end_index = 18*60;
index_offset1 = 5*60;
start_conc1 = 120 * 10(-9);
m_n1 = cleanm0n0246(:, 3);
xaxis1 = cleanm0n0246(:, 1);
baseline1 = min(m_n1);
max1 = max(m_n1);
max1b = max1;

[slope] = polyfit(xaxis1(index_offset1: end_index), m_n1(index_offset1:
    end_index), 1)

```

Here,  $k_1$  equals the estimated slope returned by the function.

Finally, after fitting the reaction rates, we fit the data to our model by adding a  $\Delta G_{k_2}^{fit}$  parameter for both the open and the closed toehold-mediated four-way branch migration cases. We found this parameter by using a minimum least squares error fit between the experimentally-fit bimolecular rates  $k_1^{fit}$  and those calculated by our model,  $k_1^{calc}$ . The main function call for the closed case is as follows:

```

ddG = 5; %estimated parameter value
[estimated_ddG] = fminunc(@forwardclosedNupackSome, ddG);

```

The error function *forwardclosedNupackSome* follows:

```

function fvalue = forwardclosedNupackSome(ddG_closed)

% k2_closed = average fit reaction rate
% N = number of steps in the branch
% k_f = forward reaction rate
% Nupack_closed = Nupack Calculated Delta G values
% exp_k = reaction rates extracted from experimental data
% k1 = reaction rate calculated by Nupack energy values adjusted by adding
    our paramter (ddG)

k2_closed= 1.5*10^-3
N = 21
k_f = 3*10^6

Nupack_closed = [-5.6000, -7.2100, -11.0300, -10.1900, -11.8000, -15.6200,
    -12.4100, -14.0200, -17.8400]
exp_k = [0.1015, 0.9329, 491.5167, 56.1973, 765.72, 277490, 9403.4, 70098,
    689780]
exp_k = log10(exp_k)

for i = 1: 9
    k1(i) = (k_f)*(k2_closed/( ((k_f)*(exp((Nupack_closed(i) + ddG)/0.593)))/N
        + k2_closed))
end

k1 = log10(k1);
fvalue = 0

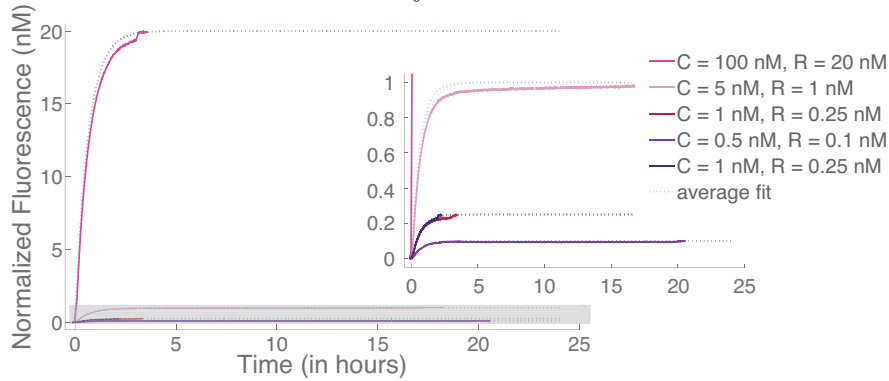
for i = 1:9
    fvalue = fvalue + (k1(i) - exp_k(i))^2    %min sum of square difference
        between simulation and data
    ddG    % outputs fitted parameter at each round
end

```

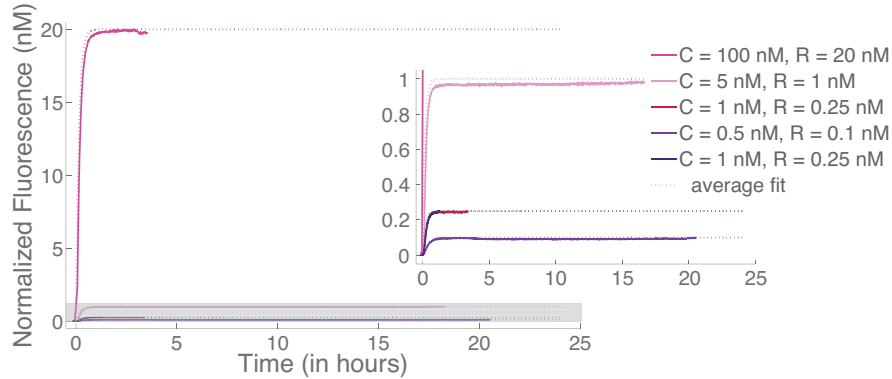


### C.3 Experimental Data

measuring  $k_2(16, 0)$   
assuming  $k_1(16, 0) = k_f$



measuring  $k_2(16, 4)$   
assuming  $k_1(16, 4) = k_f$



measuring  $k_2(16, 6)$   
assuming  $k_1(16, 6) = k_f$

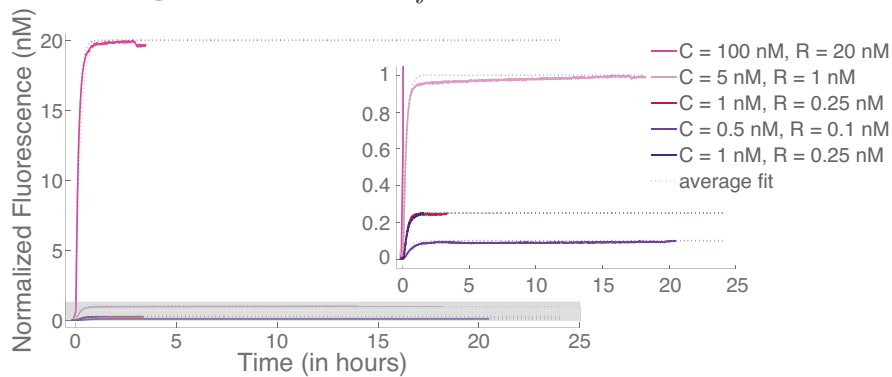
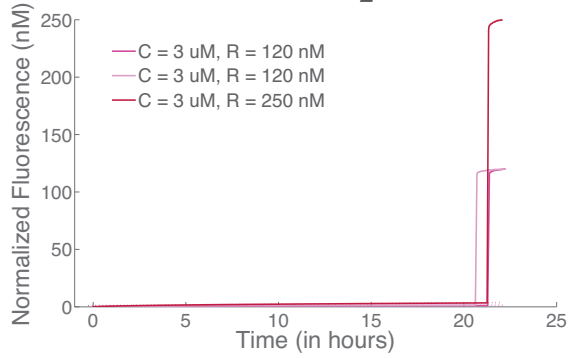
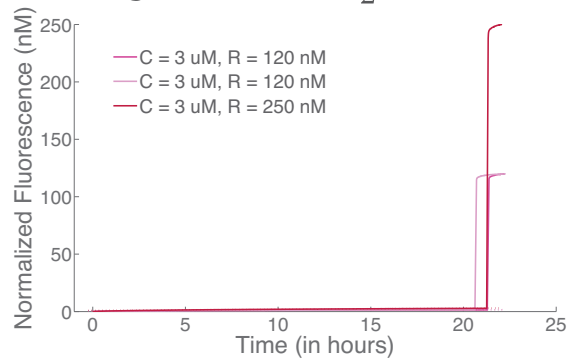


Figure C.1: Long toehold traces for fitting  $k_2$ .

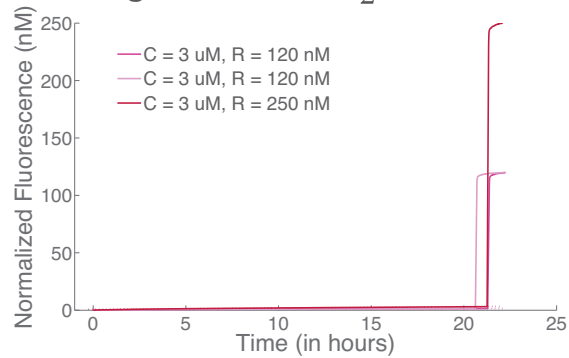
measuring  $k_1(0, 0)$   
 assuming  $k_2(0, 0) = k_2^{open}$



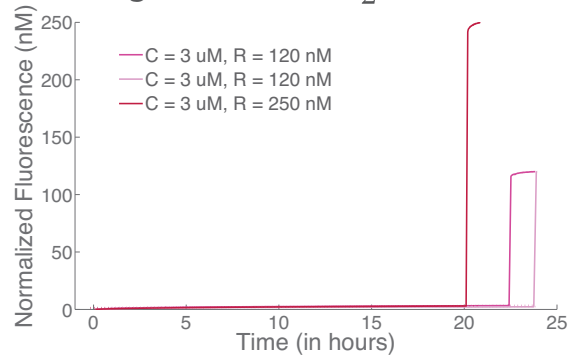
measuring  $k_1(0, 2)$   
 assuming  $k_2(0, 2) = k_2^{open}$



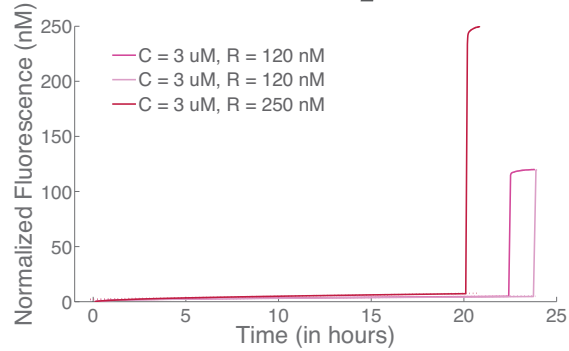
measuring  $k_1(0, 4)$   
 assuming  $k_2(0, 4) = k_2^{open}$



measuring  $k_1(2, 0)$   
 assuming  $k_2(2, 0) = k_2^{open}$



measuring  $k_1(2, 2)$   
 assuming  $k_2(2, 2) = k_2^{closed}$



measuring  $k_1(2, 4)$   
 assuming  $k_2(2, 4) = k_2^{closed}$

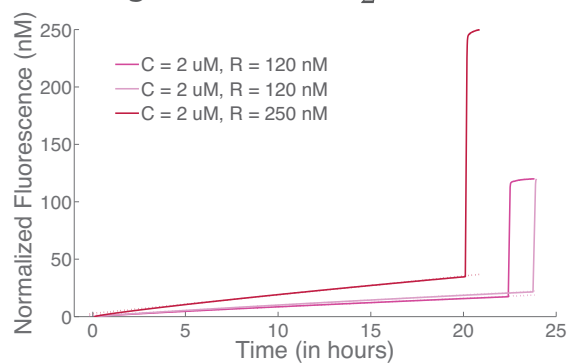
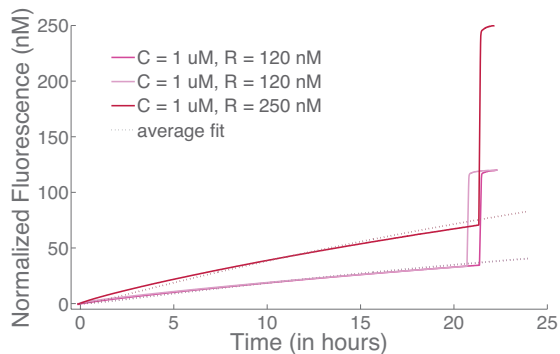
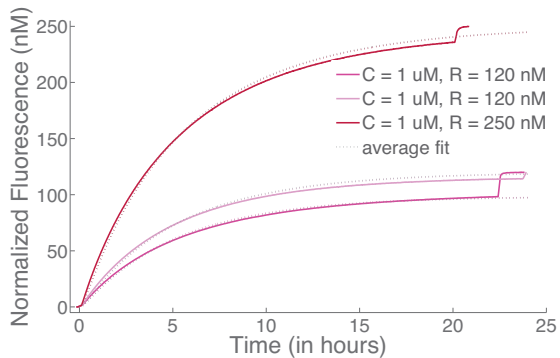


Figure C.2: Slow traces utilized a mean squared error linear fit to find  $k_1$ .

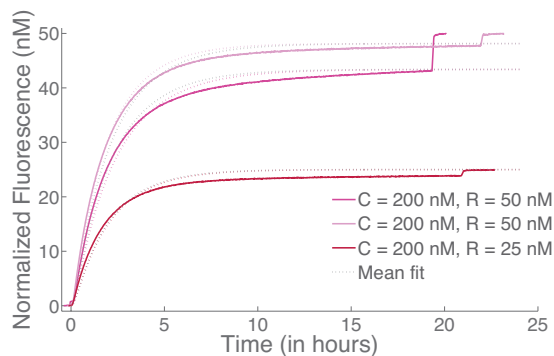
measuring  $k_1(0, 6)$   
 assuming  $k_2(0, 6) = k_2^{open}$



measuring  $k_1(4, 2)$   
 assuming  $k_2(4, 2) = k_2^{closed}$



measuring  $k_1(4, 4)$   
 assuming  $k_2(4, 4) = k_2^{closed}$



measuring  $k_1(6, 0)$   
 assuming  $k_2(6, 0) = k_2^{open}$

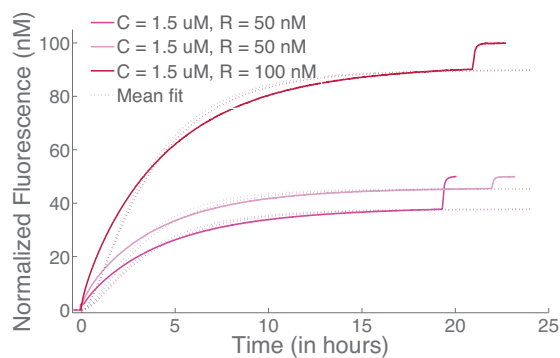


Figure C.3: Medium-speed traces utilized a mean squared error (fminunc) function to fit  $k_1$ .

### C.3.1 Completion Levels

We noted a lack of completion in our faster reactions with very low concentrations. After tracing each batch to purification date, we noticed a general trend that the older the reaction complexes, the lower the completion level (see Figures C.4, C.5, C.6, C.7). Across all batches, the variance of fitted rates is not correlated with completion level – whether the reporter was six months old or a month old, we measure the same spread of rates. Thus we are confident that our decision to fit the traces to the lowered completion level for these traces should affect the results within the standard deviation reported.

measuring  $k_1(4, 6)$   
 assuming  $k_2(4, 6) = k_2^{closed}$

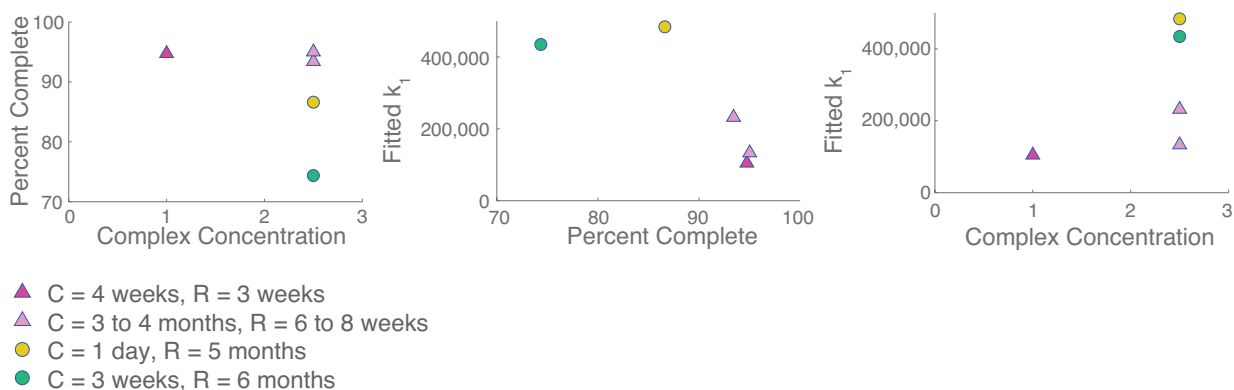
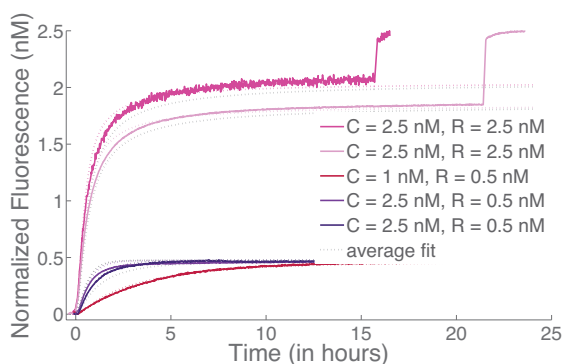


Figure C.4: We utilized a mean squared error (fminunc) function to fit  $k_1$  for the ( $m = 4, n = 6$ ) reaction. Completion levels were assessed by batch below.

measuring  $k_1(6, 2)$   
 assuming  $k_2(6, 2) = k_2^{closed}$

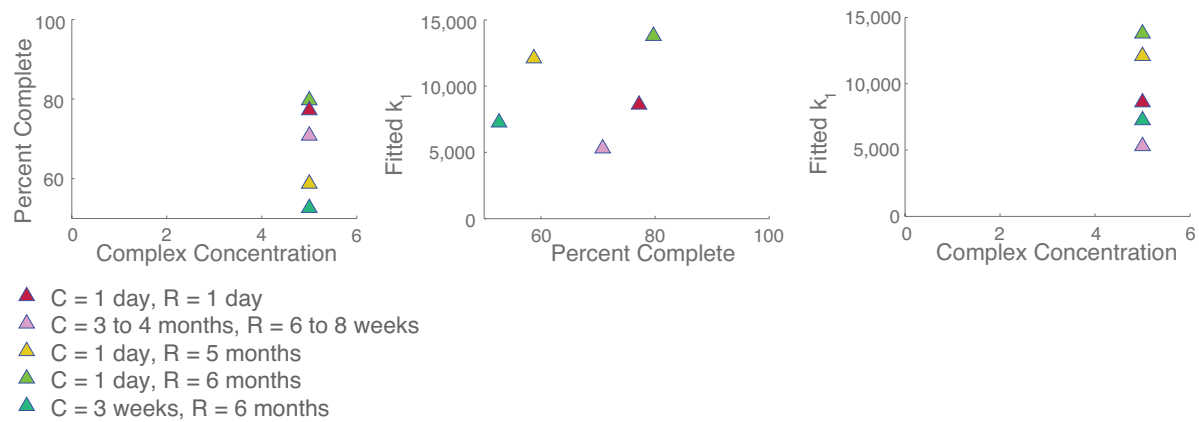
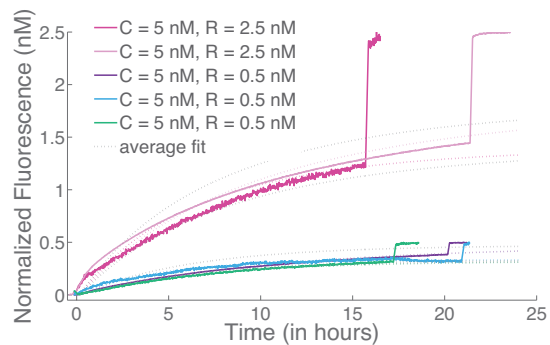


Figure C.5: We utilized a mean squared error (fminunc) function to fit  $k_1$  for the  $(m = 6, n = 2)$  reaction. Completion levels were assessed by batch below.

measuring  $k_1(6, 4)$   
 assuming  $k_2(6, 4) = k_2^{closed}$

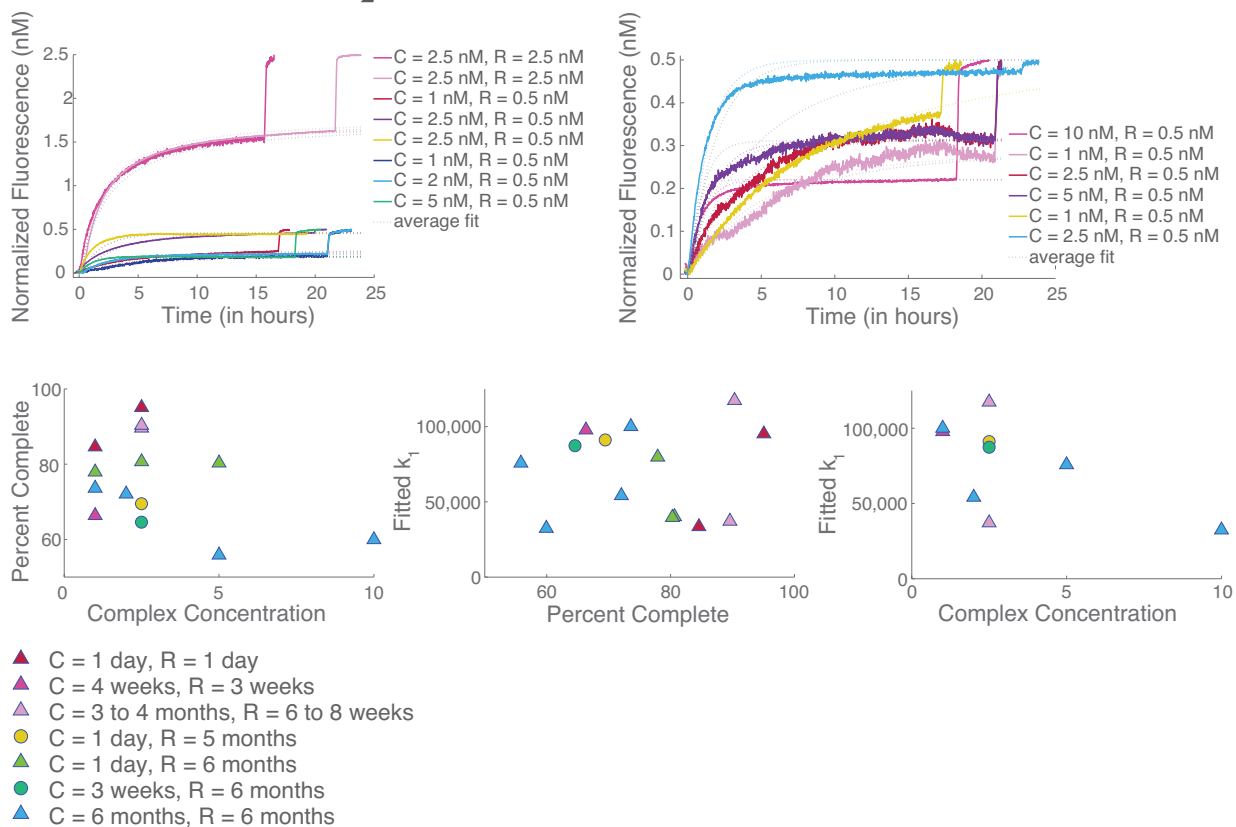


Figure C.6: We utilized a mean squared error (fminunc) function to fit  $k_1$  for the  $(m = 6, n = 4)$  reaction. Completion levels were assessed by batch below.

measuring  $k_1(6, 6)$   
 assuming  $k_2(6, 6) = k_2^{closed}$

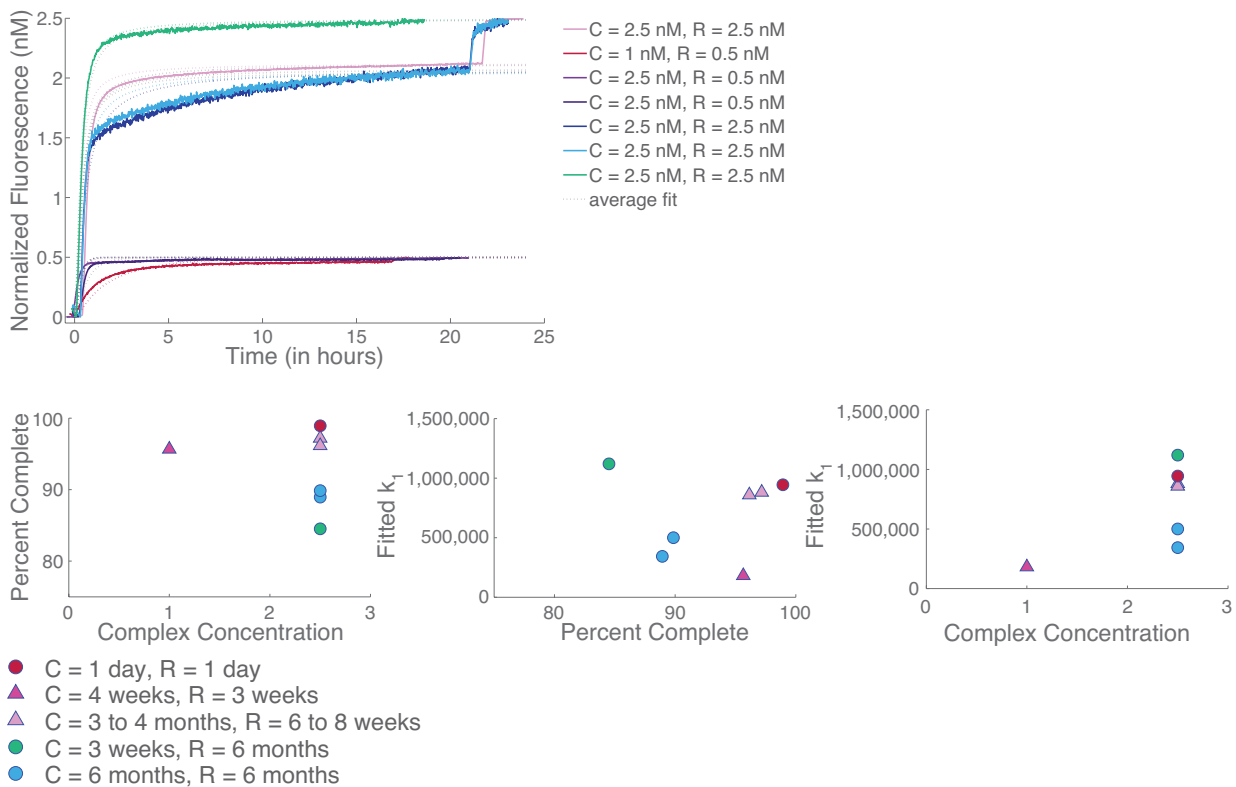
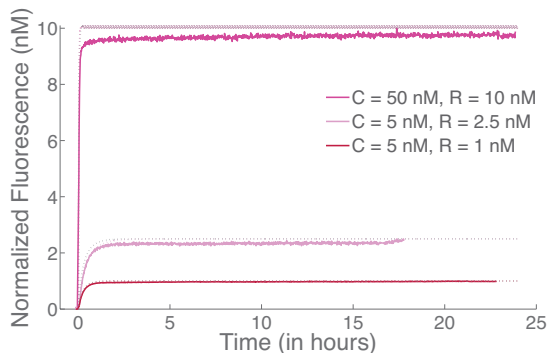


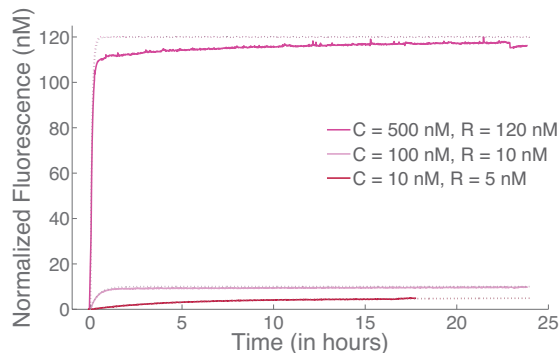
Figure C.7: We utilized a mean squared error (fminunc) function to fit  $k_1$  for the  $(m = 6, n = 6)$  reaction. Completion levels were assessed by batch below.

### C.3.2 Displacement Strand Controls

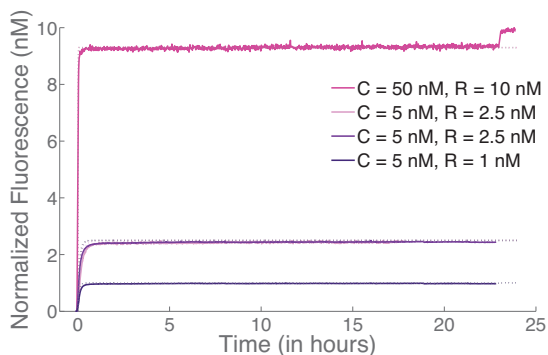
#### A m-displace -(n-toehold)



#### B n-displace -(m-toehold)



#### C m-displace +(n-toehold)



#### D n-displace +(m-toehold)

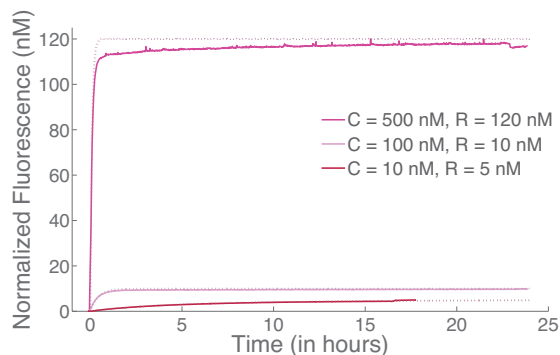


Figure C.8: (A) Reaction of m-displacement strand with a reporter complex missing the n toehold. (B) Reaction of n-displacement strand with reporter complex missing the m toehold. (C) Reaction of m-displacement strand with a reporter complex (n toehold present). (D) Reaction of n-displacement strand with a reporter complex (m toehold present).



Table C.5: Four-way Branch Migration Displacement Strand Control Concentrations

displacement strand	reporter m-toehold	reporter n-toehold	reporter concentration	displace concentration
m-displace	+	-	1 nM	5 nM
			2.5 nM	5 nM
			10 nM	50 nM
	+	+	1 nM	5 nM
			2.5 nM	5 nM
			10 nM	50 nM
n-displace	-	+	5 nM	10 nM
			10 nM	100 nM
			120 nM	500 nM
	+	+	5 nM	10 nM
			10 nM	100 nM
			120 nM	500 nM

### C.3.3 Reverse Experiments

When additional toeholds are added to the opposite side of the complex and reporter, in addition to the  $m$  and  $n$  toeholds, a reverse reaction is possible (Figure C.9). This rate will depend on the length of these toeholds in addition to the length of  $m$  and  $n$ . We gauge the significance of a reverse reaction in the case where the  $m$ -product and  $n$ -product have one complementary toehold,  $y$ , of three bases in length (Figure C.9), using the concentrations found in Table C.7. In this case the reactions most likely to go backward are  $(m = 0, n = 0)$ ,  $(m = 0, n = 2)$ ,  $(m = 2, n = 0)$ .

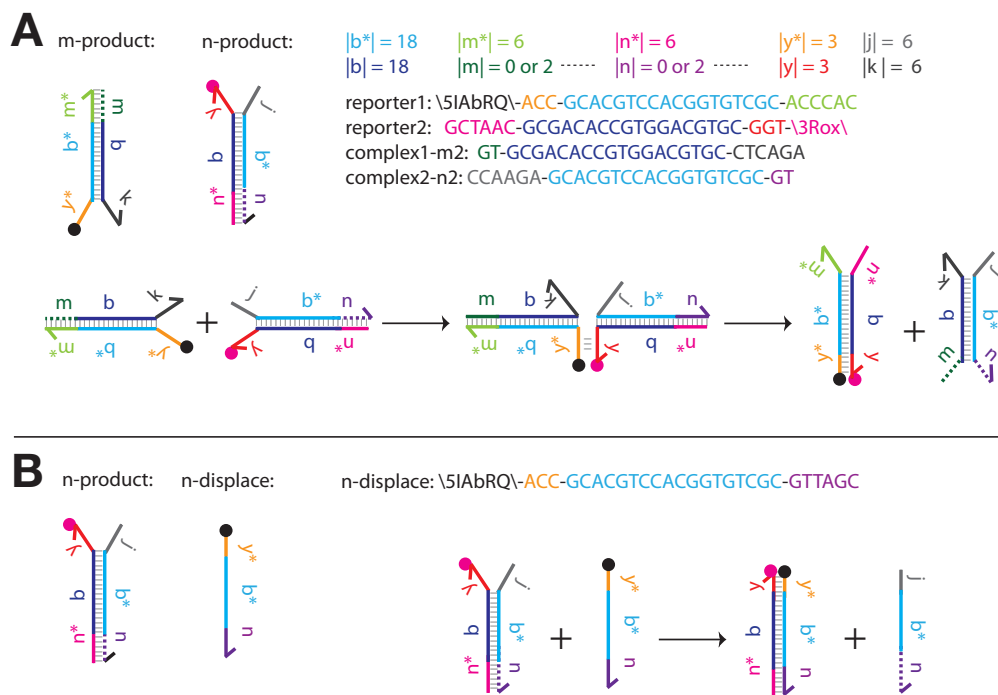


Figure C.9: (A) Experimental set-up to measure reverse reaction rates: We annealed and purified the product complexes ( $m$ -product and  $n$ -product) with a  $y$  and  $y'$  toehold domain of three base pairs and an extra toehold that is not complementary to anything in solution. This reverse reaction would be equivalent to a forward reaction with toeholds of length  $(m = 0, n = 3)$ . If the two complexes react and complete strand exchange, regenerating the original Reporter and Complex, we expect the overall fluorescence in solution to decrease. Sequences for DNA strands are color-coded by domain, \5IAbRQ\ indicates a 5' Iowa Black red quencher modification, and \3Rox\ indicates a 3' ROX fluorophore modification. (B) At the end of the experiment another strand of DNA is added into the solution in order to fully displace all unreacted complexes. In contrast to the experiments discussed in the main paper this displacement strand has a 5' quencher modification, thus when added in excess the fluorescence levels quickly decrease. As above, sequences are color-coded by domain.

Table C.7: Reverse Four-way Branch Migration Experimental Concentrations

toehold length	m-product concentration	n-product concentration
m = 0, n = 0	1 $\mu$ M	500 nM
m = 0, n = 2	1 $\mu$ M	500 nM
m = 2, n = 0	1 $\mu$ M	500 nM

Table C.6: Reverse experiment sequences

reporter1	\5IAbRQ\ -ACC-GCACGTCCACGGTGTTCGC-ACCCAC
reporter2	GCTAAC-GCGACACCGTGGACGTGC-GGT-\3Rox\
complex-m2	GT-GCGACACCGTGGACGTGC- CTCAGA
complex-m0	GCGACACCGTGGACGTGC- CTCAGA
complex-n2	CCAAGA- GCACGTCCACGGTGTTCGC-GT
complex-n0	CCAAGA- GCACGTCCACGGTGTTCGC
n-displace	\5IAbRQ\ -ACC-GCACGTCCACGGTGTTCGC-GTTAGC

In these experiments the two product complexes (m-product and n-product) were annealed, each complex had a three-base-toehold on the opposite end of the complex from the m and n toehold sites. Because the product complexes separate the fluorophore quencher pair, the progress of this reaction is observed in reverse: we expect that if the reverse reaction occurs it will result in the reactants of our original experiments: the Reporter and Complex. In the newly formed Reporter, the fluorophore and quencher will be paired again resulting in an over-all decrease in fluorescence. At the end of the experiment another strand of DNA is added into the solution in order to fully displace all unreacted complexes. In contrast to the experiments discussed in the main paper this displacement strand has a 5' quencher modification, thus when added in excess the fluorescence levels quickly decrease (Figure C.9B).

The reverse reactions in our smallest toehold cases were negligible (Table C.8 and Figure C.10). Since these were the most energetically favorable of all of the reverse reactions, we are confident that the effect of a reverse reaction on our kinetics experiments is negligible.

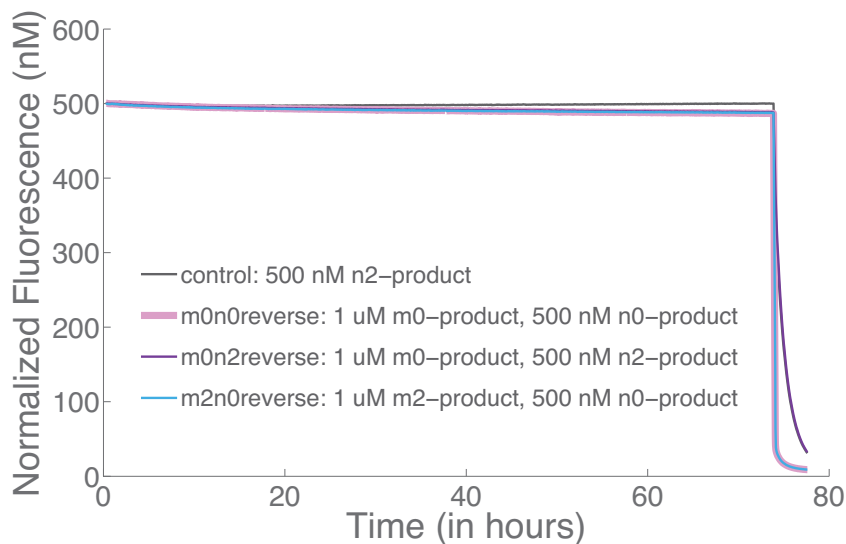


Figure C.10: Reversible four-way branch migration traces to fit the value of  $k_r(0, 3)$ .

Fitted $k_r$ Rates for reversible four-way branch migration	
toehold length	average $k_r(0, 3)$ ( $sec^{-1}$ )
control	$\approx 0$
m0n0	0.11
m0n2	0.096
m2n0	0.093

Table C.8: Reverse reaction rate determined by linear fitting to experimental traces of reversible four-way branch migration. The control (500 nM n-product solution) showed a negligible change in fluorescence over three days resulting in an observed rate of:  $k_r^{fit}(0, 3) = -0.025$  ( $sec^{-1}$ ), which we interpret as zero within experimental error.

## C.4 Reaction Coordinate

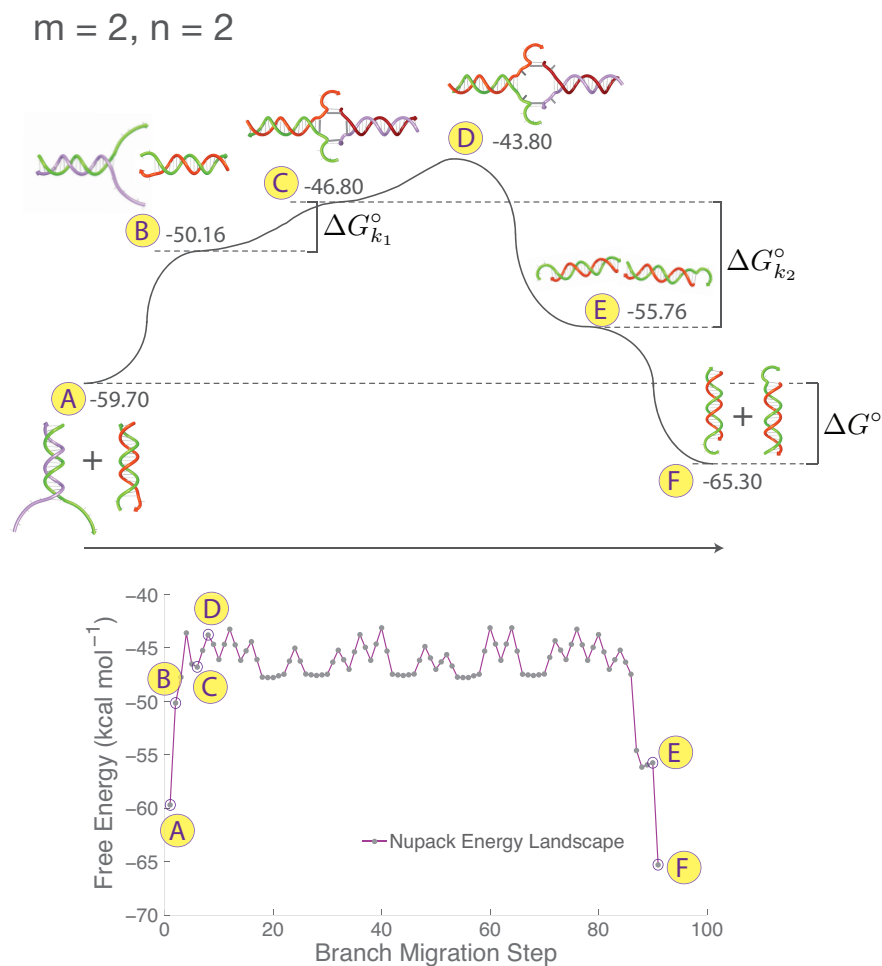


Figure C.11: A reaction coordinate for the open loop case where ( $m = 2, n = 2$ ). It is accompanied by a Nupack simulation of one trajectory of the thermodynamic energy landscape; each point indicates the formation or cleavage of a single hydrogen bond. Labels correspond to the indicated state in reaction coordinate. Equations are listed in Figure 5.4.

## C.5 Trajectory Simulations

Simulated reaction rates ( $k_1^{sim}$ ) were calculated using Multistrand [Schaeffer, 2012], an analysis tool that simulates the kinetics of multistranded DNA systems with single-basepair resolution utilizing the NUPACK energetics model. Sample size indicates the number of trajectories simulated.

Final values were normalized by computing a scaling factor by minimizing the mean multiplicative factor that best fit the raw multistrand results to the experimental results, which in this case was a factor of 20. Values that are upper-bounded indicate reactions that did not have a single forward result.

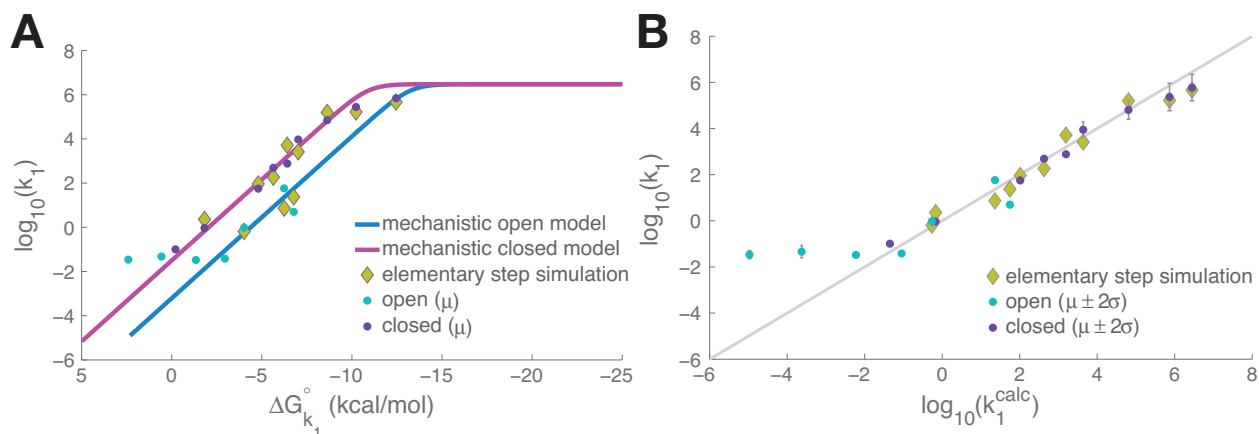


Figure C.12: Multistrand-determined reaction rates  $k_1^{sim}$  (yellow diamonds) are plotted against, experimentally fit and calculated rates. (A) Plot of  $\Delta G_{k_1}^{\circ}$  versus  $\log_{10}(k_1)$  compares our models for open (blue) and closed (magenta) loop toehold-mediated four-way branch migration to our experimentally fit mean  $k_1$  rates; dots correspond to open (blue) and closed (purple) loop reactions. (B) Plot compares the  $\log_{10}(k_1)$  rate calculated by our model to the experimentally fit mean rates. Error bars show two standard deviations of error in our experimental measurements.